High-energy neutrino-nucleon deep inelastic scattering

Keping Xie

Department of Physics and Astronomy,
Michigan State University, East Lansing, MI 48824

Fermilab Neutrino Seminar
March 14, 2024

In collaboration with Jun Gao (SJTU), Tim Hobbs (Argonne),
Daniel Stump and C.-P. Yuan (MSU)

[arXiv:2303.13607]

Outline

Neutrino Sources

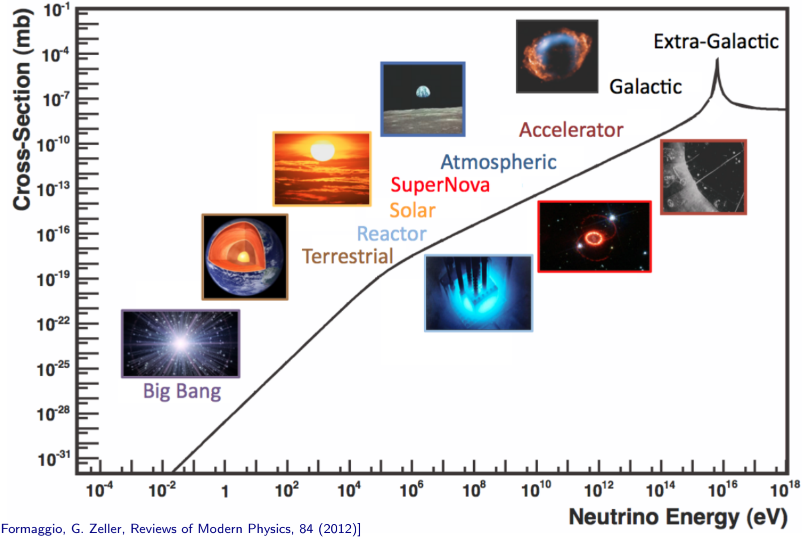

[J. A. Formaggio, G. Zeller, Reviews of Modern Physics, 84 (2012)]

- We focus on (ultra-)high-energy neutrinos, mainly from Galactic plane.
- Some accelerator neutrinos can reach intermediate high energies ($\gtrsim 10$ GeV)

Neutrinos at IceCube(-Gen2)

[2204.04237]

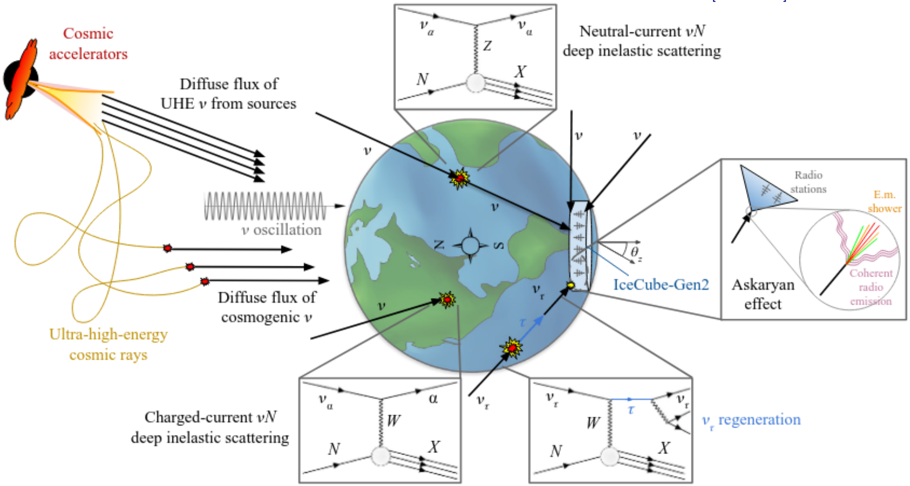

Many neutrino observatories (under development)

- IceCube-Gen2 [2008.04323]
- KM3NeT [1601.07459]
- Baikal-GVD [Nucl. Instrum. Meth. A, 11']
- GRAND [1810.09994]
- POEMMA [1708.07599]
- P-ONE [2005.09493]
- TRIDENT [2207.04519]

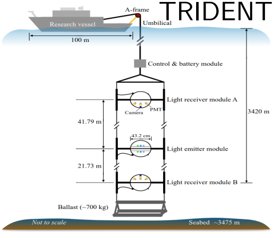

IceCube-Gen2

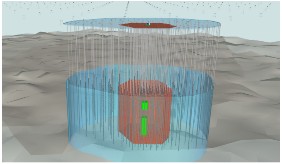

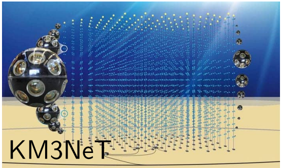

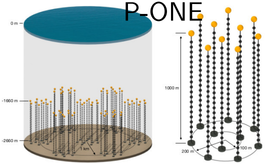

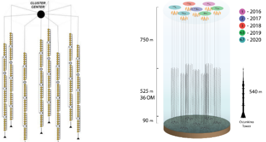

Baikal-GVD

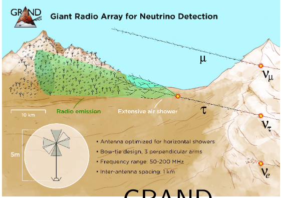

GRAND

Neutrino-electron scattering

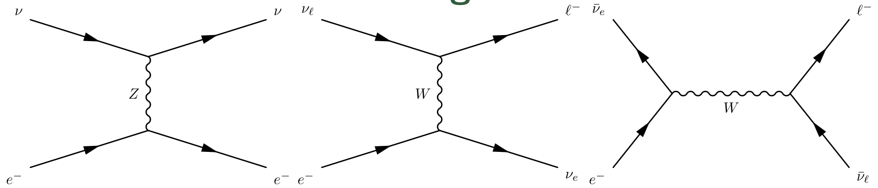

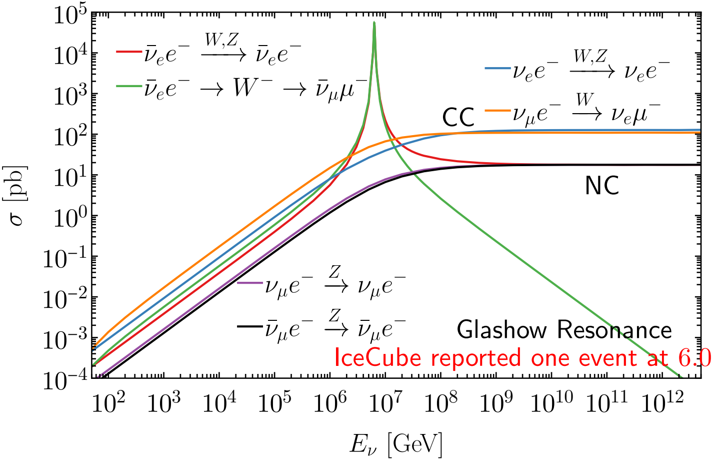

[Nature 21']

IceCube reported one event at 6.05 ± 0.72 PeV

Neutrino-nucleon Interactions

Charged-Current (CC) interactions via W boson

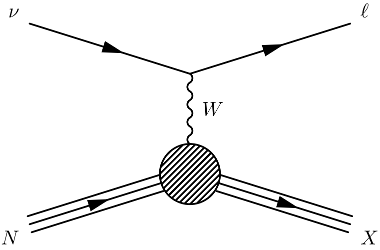

Neutral-Current (NC) interactions via Z boson

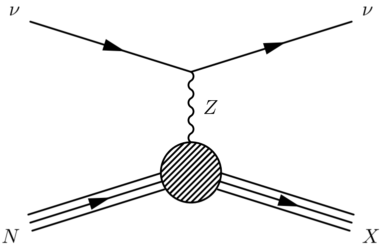

Charged-Current interactions

Quasi-elastic scattering (QE)

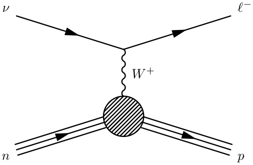

Resonance production (RES)

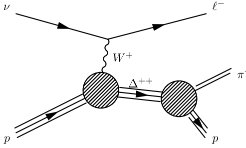

Deeply inelastic scattering (DIS)

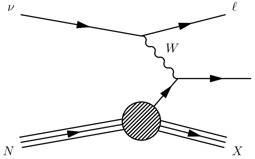

Total neutrino and antineutrino per nucleon CC cross sections

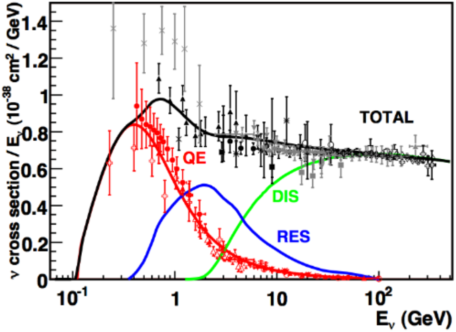

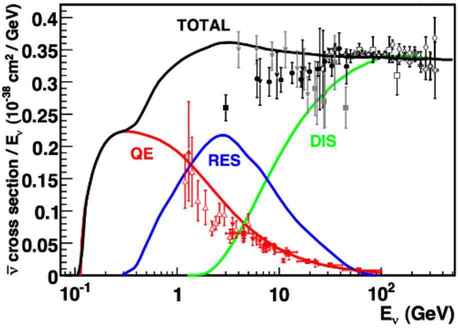

[J. A. Formaggio, G. Zeller, Reviews of Modern Physics, 84 (2012)][hep-ph/0208030]

Neutrino-Nucleon CC cross sections

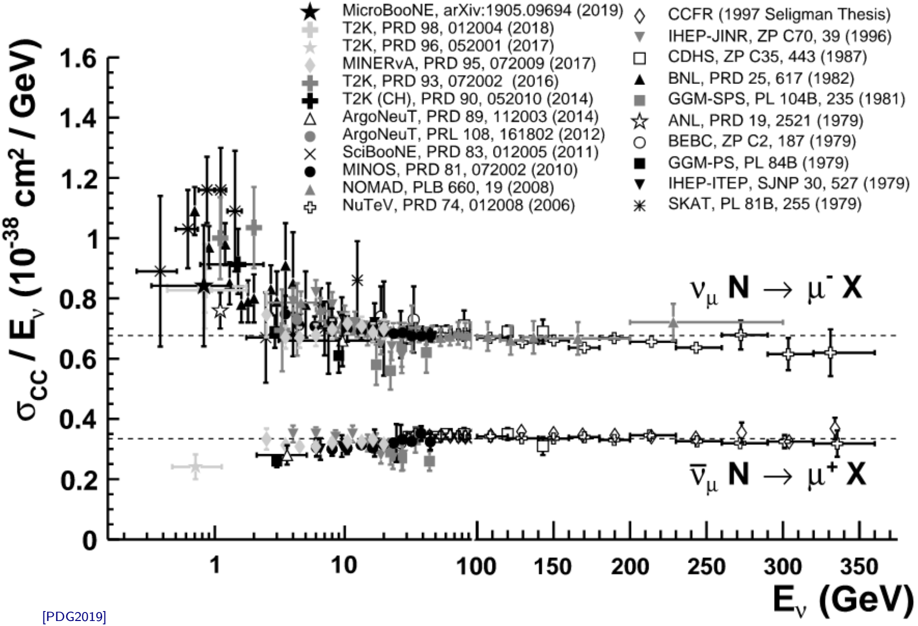

[PDG2019]

High-energy neutrino measurements

[2204.04237]

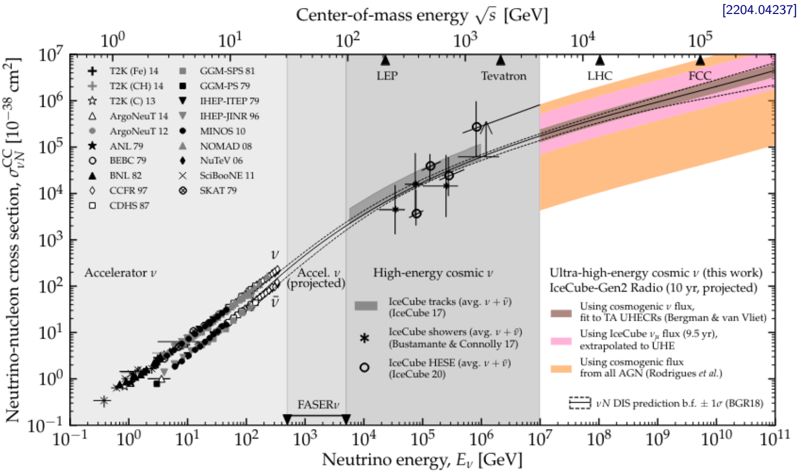

- High energy neutrinos: colliders
- Ultrahigh energy neutrinos: astrophysical source

IceCube cross sections

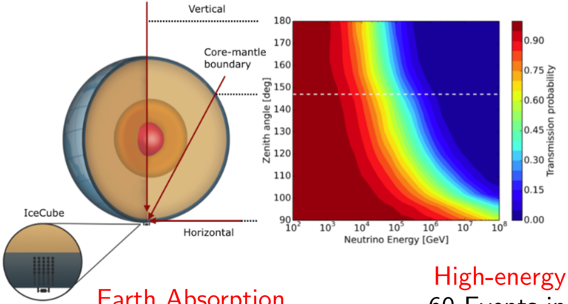

Earth Absorption

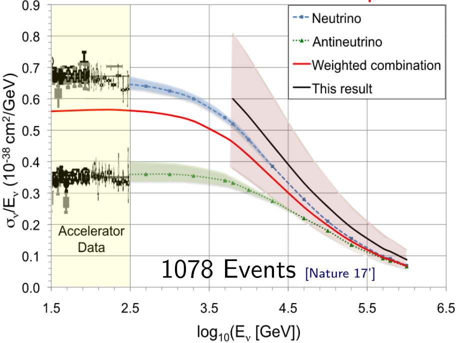

1078 Events [Nature 17']

High-energy Starting Event

60 Events in 7.5 years [PRD 21']

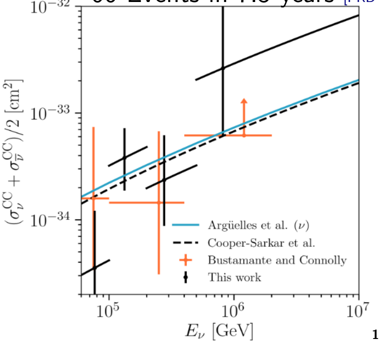

The neutrino-nucleon DIS cross section

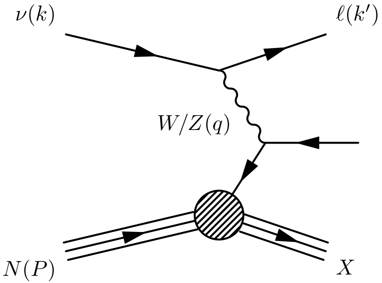

Kinematic variables

$$Q^2 = -q^2 = -m_\ell^2 + 2E_\nu(E' - k'\cos\theta) \tag{1}$$

$$x = \frac{Q^2}{2P\cdot q} = \frac{Q^2}{2M(E_\nu - E')}, \quad y = \frac{P\cdot q}{P\cdot k} = \frac{E_\nu - E'}{E_\nu} = \frac{Q^2}{2xME_\nu}, \tag{2}$$

Inclusive cross section

$$\frac{\mathrm{d}^2\sigma^{\nu(\bar{\nu})}}{\mathrm{d}x\mathrm{d}y} = \frac{G_F^2 M E_\nu}{\pi\left(1 + Q^2/M_{W,Z}^2\right)^2}\left[\begin{array}{c} \frac{y^2}{2}2xF_1\left(x,Q^2\right) + \left(1 - y - \frac{Mxy}{2E}\right)F_2\left(x,Q^2\right) \\ \pm y\left(1-\frac{y}{2}\right)xF_3\left(x,Q^2\right)\end{array}\right] \quad (3$$

Structure Functions in the parton model (LO)

Callan-Gross relation

$$F_L^V = F_2^V - 2xF_1^V = 0,\;\; V = \gamma, Z, \gamma Z, W^\pm. \tag{4}$$

Neutral Current

$$\begin{aligned}\left[F_2^\gamma, F_2^{\gamma Z}, F_2^Z\right] &= x\sum_q \left[e_q^2, 2e_q g_V^q, g_V^{q\,2} + g_A^{q\,2}\right](q+\bar{q}) \\ \left[F_3^\gamma, F_3^{\gamma Z}, F_3^Z\right] &= \sum_q \left[0, 2e_q g_A^q, 2g_V^q g_A^q\right](q-\bar{q}),\end{aligned} \tag{5}$$

where

$$g_V^q = \pm\frac{1}{2} - 2e_q \sin^2\theta_W,\;\; g_A^q = \pm\frac{1}{2}. \tag{6}$$

Charged Current

$$\begin{aligned}F_2^{W^-} &= 2x(u+\bar{d}+\bar{s}+c\ldots), \\ F_3^{W^-} &= 2(u-\bar{d}-\bar{s}+c\ldots),\end{aligned} \tag{7}$$

Kinematic Phase space

The DIS inclusive cross section

$$\sigma = \int_{Q^2_{\min}}^{2ME_\nu} \mathrm{d}Q^2 N\left(Q^2\right) \int_{Q^2/(2ME_\nu)}^{1} \frac{\mathrm{d}x}{x} \mathscr{F}[F_{i=1,2,3}]\left(x, Q^2\right). \quad (8)$$

Integration limits

$$Q^2 \in [Q^2_{\min}, 2ME_\nu],\ x \in [Q^2/(2ME_\nu), 1]. \quad (9)$$

Experiments can select the DIS events, such as $Q_{\min} = 1$ GeV in MINERvA [1601.06313].

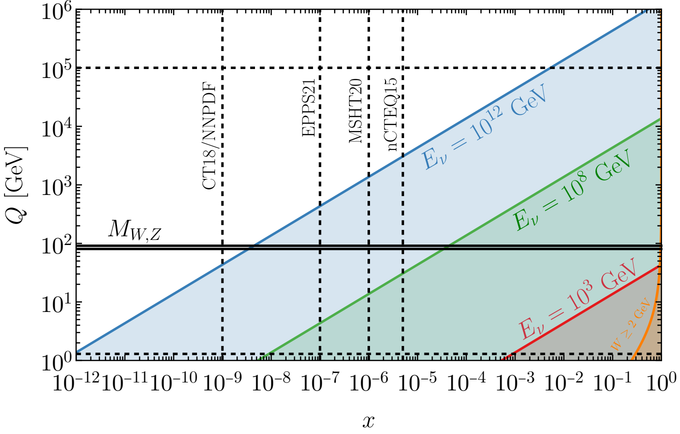

The data probed (x, Q) region [1912.10053]

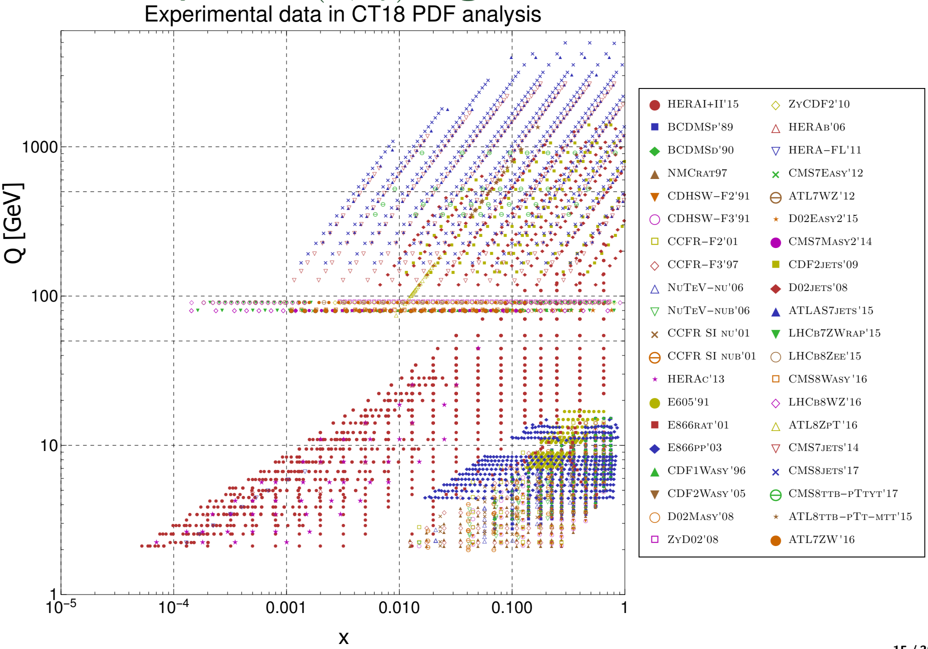

Small-x PDFs: Extrapolation vs Evolution

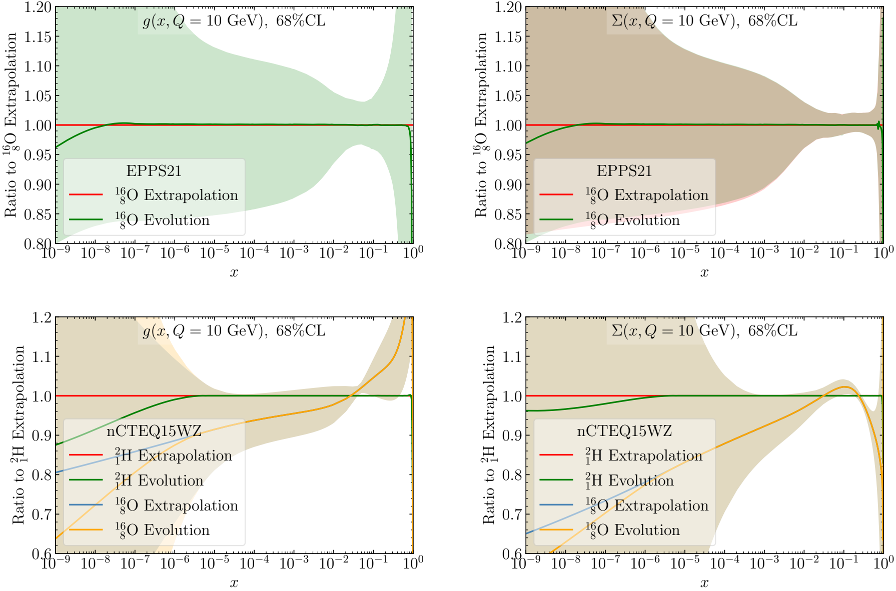

PDFs at $Q < Q_0$ and $x < x_{\mathrm{min}}$

- Extrapolation: LHAPDF
- Backward evolution: APFEL

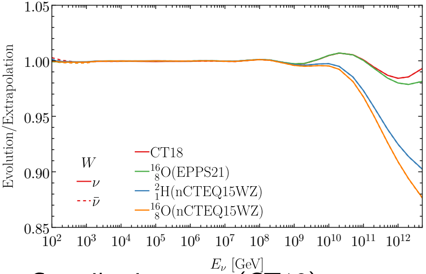

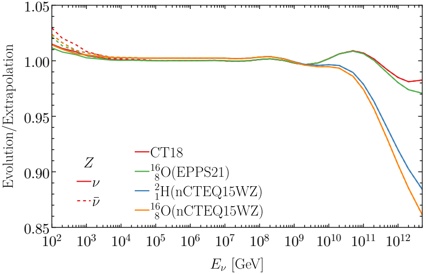

Contribution to σ (CT18)

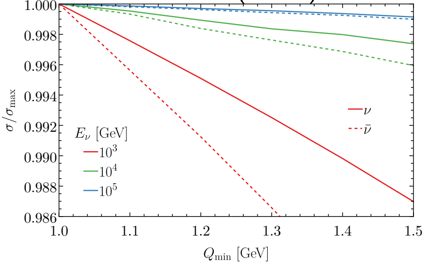

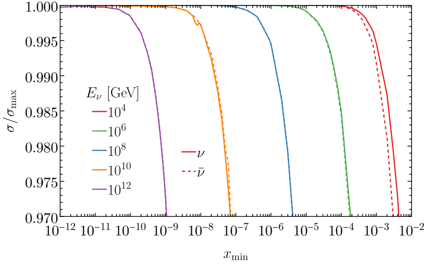

Dominant integration region of (x, Q^2)

- Dominant integration region: $Q \sim M_{W,Z}, x \sim M_{W,Z}^2/(2ME_\nu)$

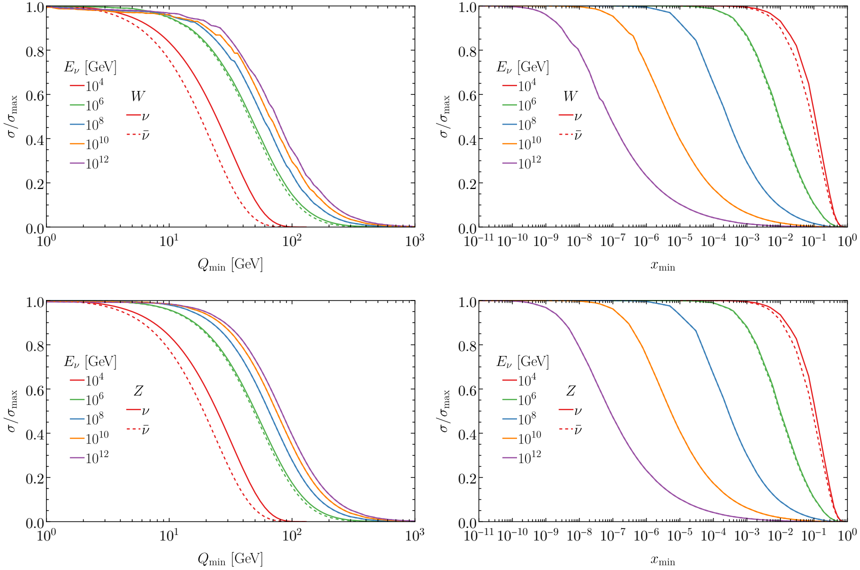

2D contours

Integrate the trapezoidal region

$$\int_{Q^2_{\min}}^{2ME_\nu} \mathrm{d}Q^2 \int_{\max\left(\frac{Q^2}{2ME_\nu}, x_{\min}\right)}^{1} \mathrm{d}x \qquad (10)$$

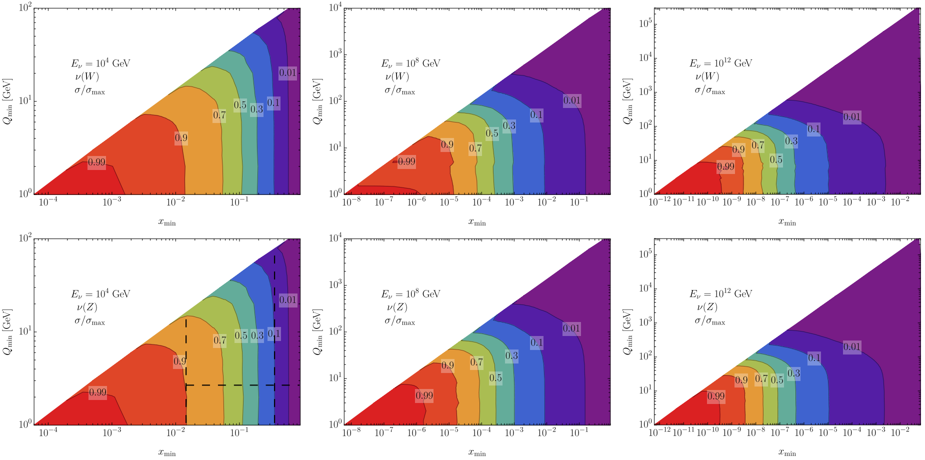

See backup slides for $\bar{\nu}$ cross sections.

PDF correlation

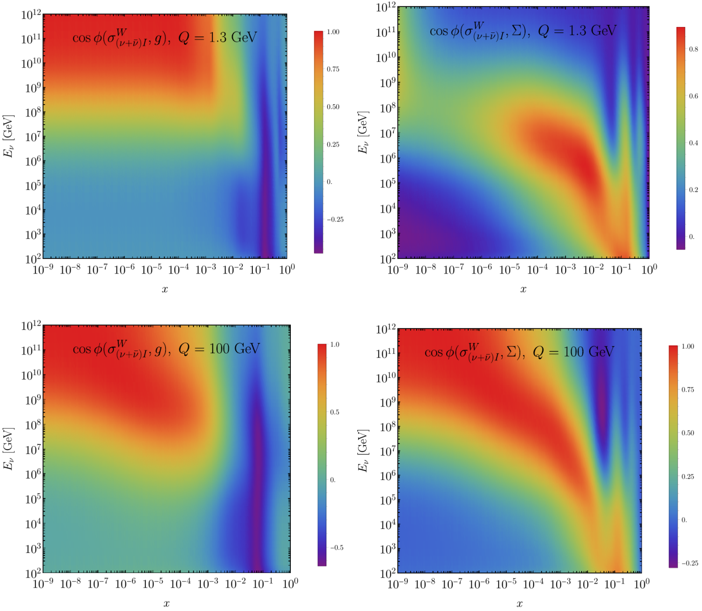

- The singlet $x \sim M^2_{W,Z}/(2ME_\nu)$
- At high Q, $\Sigma \leftrightarrow g$ correlated.

QCD corrections

- QCD factorization:

$$F(x,Q^2) = \sum_i \int_x^1 \frac{\mathrm{d}z}{z} C_i\left(\frac{x}{z}, \frac{Q^2}{\mu_f^2}, \alpha_s\right) f_i(z,\mu_f^2) + \mathscr{O}\left(\frac{\Lambda^2}{Q^2}\right), \tag{11}$$

  where i indicates parton $q, \bar{q}, g$.

- PDF evolution – DGLAP

$$\frac{\mathrm{d}f_i(x,\mu_f^2)}{\mathrm{d}\log\mu_f^2} = \sum_j \int_x^1 \frac{\mathrm{d}z}{z} P_{ij}\left(\frac{x}{z}\right) f_j(z,\mu_f^2). \tag{12}$$

- Perturbative expansion of Wilson coefficients

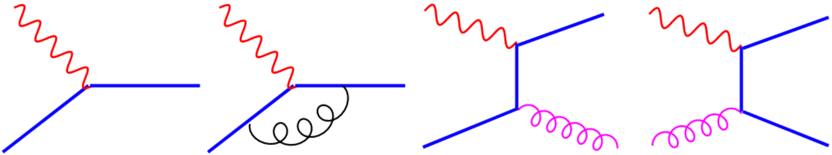

- Heavy-quark mass effect [More comes later].
  - $Q^2 \sim m_q^2$: Fixed-Flavor-Number scheme, Flavor Creation
  - $Q^2 \gg m_q^2$: Zero-Mass, Flavor Excitation

Perturbative orders up to N3LO

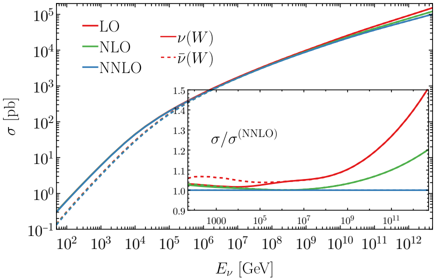

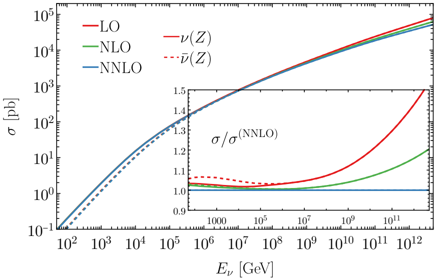

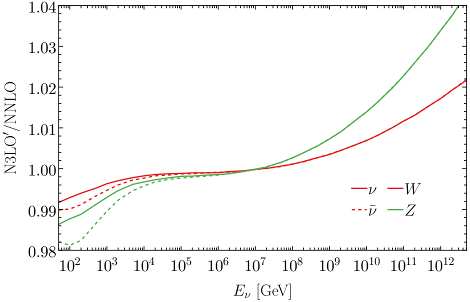

[CT18LO:2205.00137]

[CT18(N)NLO:1912.10053]

- LO/NLO/NNLO: $C^{(0/1/2)} \otimes f^{(0/1/2)}$
- N3LO′: $C^{(3)} \otimes f^{(2)}$ [ZM WC:[arXiv:0504242,0708.3731,0812.4168], [more recently:1606.08907,2208.14325]

General-Mass Variable-Flavor-Number scheme

- Master Formula: ACOT matching [Aivazis, Collins, Olness, Tung, PRD1994]

$$\mathrm{ACOT} = \mathrm{FC} + \mathrm{FE} - \mathrm{Sub.} \tag{13}$$

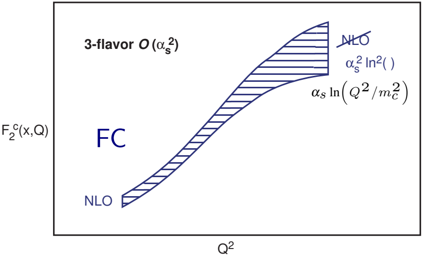

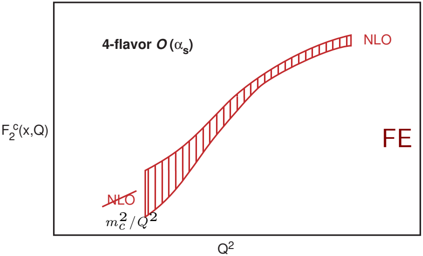

General-Mass Variable-Flavor-Number scheme

- Master Formula: ACOT matching [Aivazis, Collins, Olness, Tung, PRD1994]

$$\mathrm{ACOT} = \mathrm{FC} + \mathrm{FE} - \mathrm{Sub.} \tag{13}$$

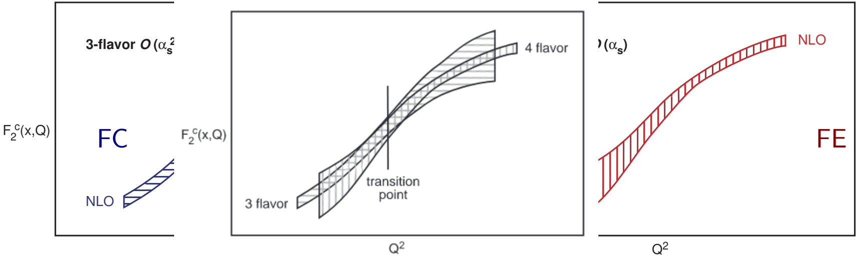

- Asymptotic behaviors
  - $Q \gtrsim m_c$, m_c matters, $f_c(x, \mu^2) \approx 0$, FE∼Sub, FC dominates (FFN 3-flv).
  - $Q \gg m_c$, $m_c \approx 0$, $f_c(x, \mu^2)$ matters, FC∼Sub, FE dominates (ZM 4-flv).
- The Simplified ACOT scheme: treats heavy-quark as massless in Flavor Excitation [Collins, PRD1998, Kramer PRD2000].
- The S-ACOT scheme at NNLO for DIS: NC [Guzzi, 1108.5112], CC [Gao, 2107.00460].

General-mass variable-flavor-number scheme

Quark mass effect [1108.5112,2107.00460]

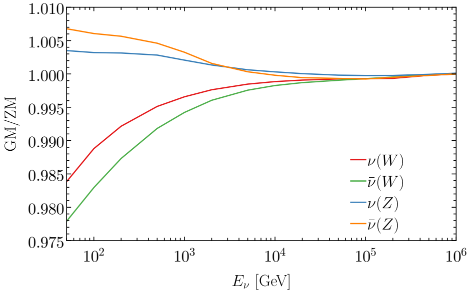

Variable flavor numbers

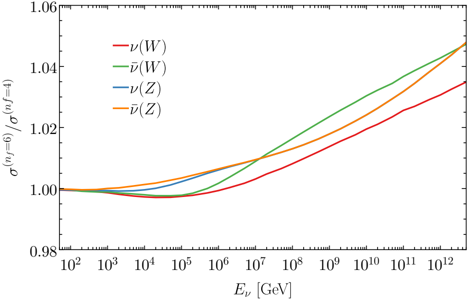

PDFs at small x

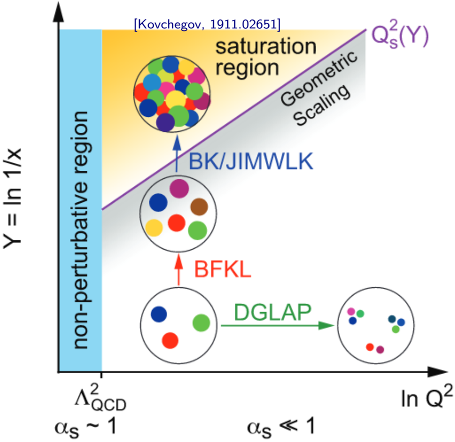

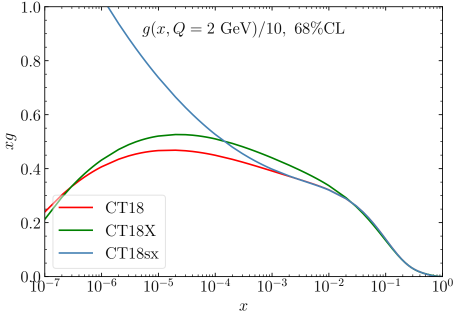

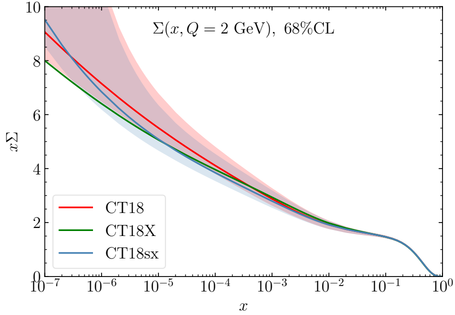

- CT18X [1912.10053] takes a saturation model: x-dependent DIS scale
- CT18sx [2108.06596] resum the $\ln(1/x)$ with BFKL (HELL package [1607.02153,1708.07510])

Small-x resummation

- Perturbative Wilson coefficient and splitting functions contains $\ln(1/x)$ (single-log enhanced)

$$C(x,\alpha_s)[\text{ or } P(x,\alpha_s)] = a_0 + \alpha_s\left[a_1\ln(1/x) + b_1\right] + \alpha_s^2\left[a_2\ln^2(1/x) + b_2\ln(1/x) + c_2\right] + \cdots$$

- Large $\alpha_s\ln(1/x)$ spoils the perturbative convergence $\Longrightarrow$ resummation
- DGLAP vs BFKL: $\xi = \ln(1/x)$ and $t = \ln\left(Q^2/\Lambda^2\right)$.

$$g(N,t) = \int_0^\infty d\xi\, e^{-N\xi} g(\xi,t) \quad \Longrightarrow \frac{d}{dt}g(N,t) = \gamma(N,\alpha_s)g(N,t),$$

$$g(\xi,M) = \int_{-\infty}^\infty dt e^{-Mt} g(\xi,t) \quad \Longrightarrow \frac{d}{d\xi}g(\xi,M) = \chi(M,\alpha_s)g(\xi,M).$$

- Match the DGLAP with the BFKL [HELL: 1607.02153,1708.07510]

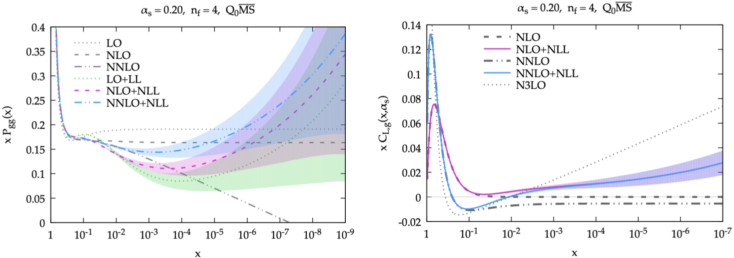

Impacts on structure functions

[2108.06596]

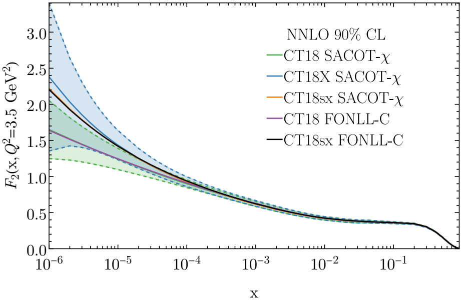

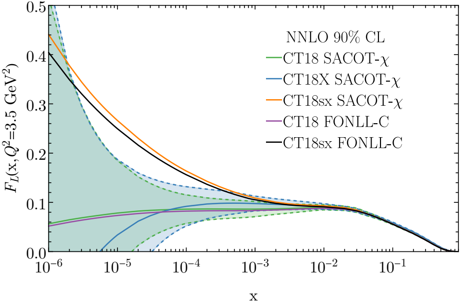

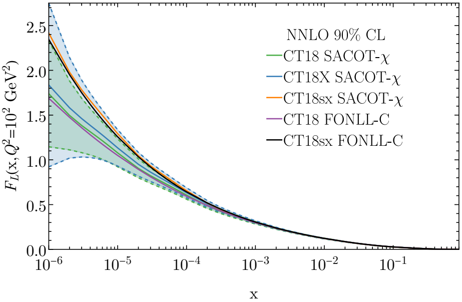

- Both CT18X and CT18sx enhance the F_2 at small x and Q.
- CT18X reduces F_L at small x while CT18sx enhances F_L.
- Both effects disappear at Q.

$$F_2^{\mathrm{NLLx,SACOT}} = \underbrace{\frac{C(\mathrm{NLLx})\otimes f(\mathrm{CT18sx})}{C(\mathrm{NNLO})\otimes f(\mathrm{CT18})}}_{K:\ \mathrm{FONLL-C}} \underbrace{C(\mathrm{NNLO})\otimes f(\mathrm{CT18})}_{F_2^{\mathrm{SACOT}}(\mathrm{CT18})}$$

Impacts on cross sections

- The BFKL resummation of small-x (large $\log x$) enhances (reduces) gluon (flavor singlet) PDFs at low Q^2 (HELL [1607.02153,1708.07510]).
- Typical x

$$x_{W,Z} = \frac{M_{W,Z}^2}{2ME_\nu} \sim 10^{-5} \implies E_\nu \sim 10^9 \text{ GeV}.$$

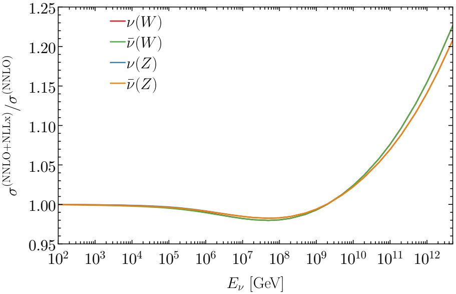

Predictions for neutrino-isoscalar cross sections

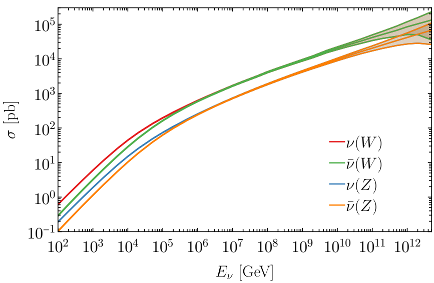

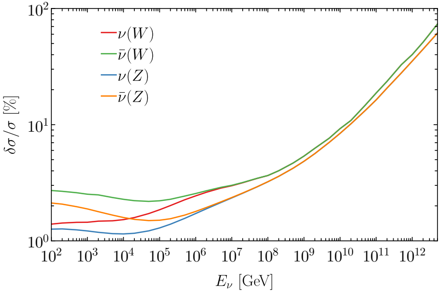

- Exact NNLO (full mass dependence [1108.5112,2107.00460]), while N3LO ZM WC [1606.08907,2208.14325]
- $n_f = 6$ Flavors
- Small-x resummation

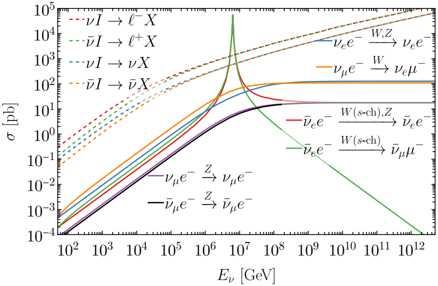

PDF comparison

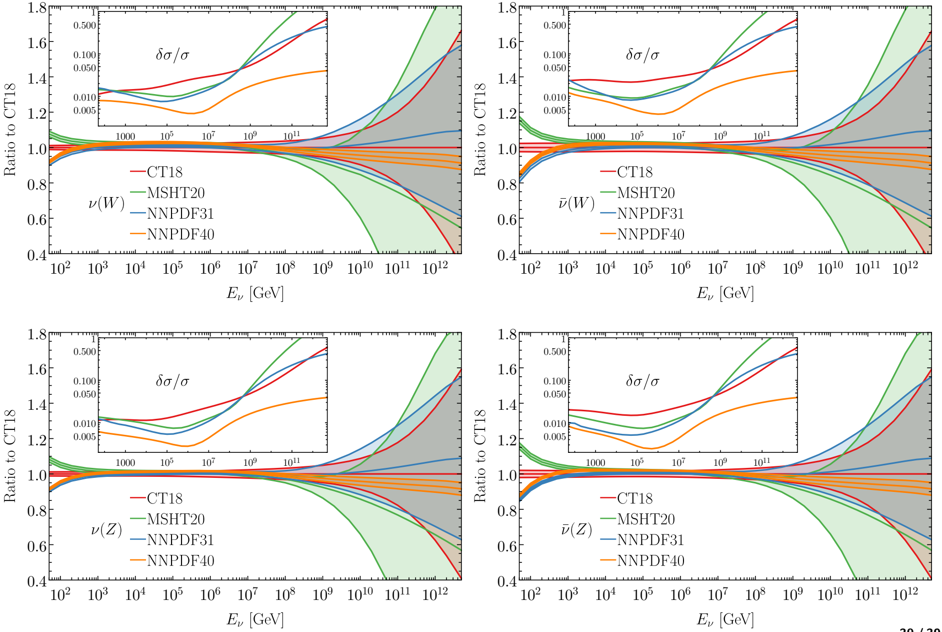

Other calculations

- Gandhi-Quigg-Reno-Sarcevic [hep-ph/9807264]: CTEQ4M, LO
- Connolly-Thorne-Waters [1102.0691]: MSTW08, LO
- Cooper-Sarkar-Mertsch-Sarkar [1106.3723]: HERAPDF1.5, NLO (IceCube)
- Argüelles-Halzen-Wille-Kroll-Reno [1504.06639]: Color dipole model
- Bertone-Gauld-Rojo [1808.02034,2004.04756]: NNPDF3.1sx, NNLO (NLO in Genie)
- NNSFν [2302.08527]: Bodek-Yang model, NNPDF4.0, NNLO
- Jeong-Reno [2307.09241]: Shallow inelastic scattering

Comparison with the CSMS calculation (IceCube)

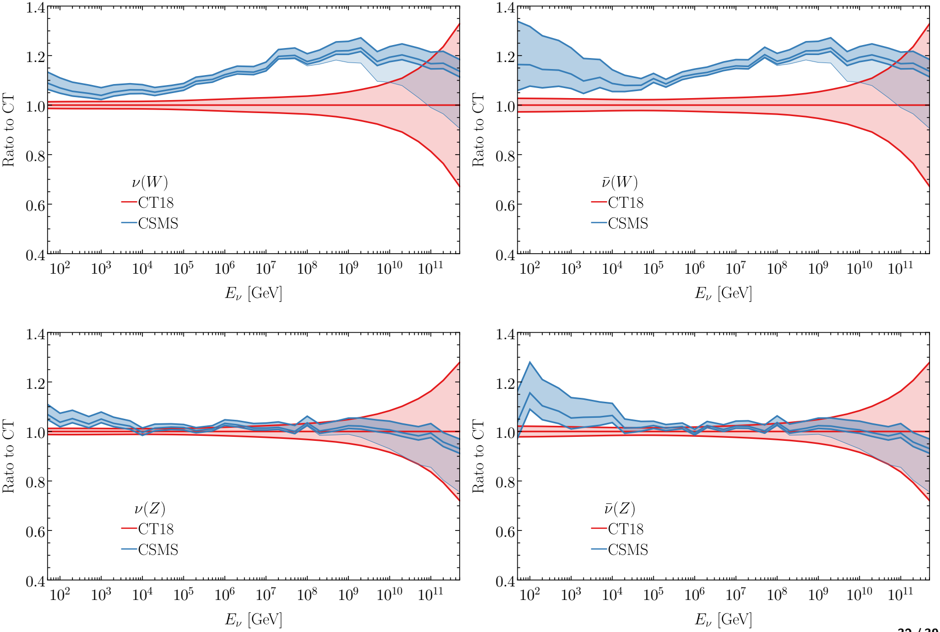

Nuclear impacts (simplified)

- The water nucleon number averaged cross sections:

$$F_i^{\mathrm{H_2O}} = \frac{1}{2+A}(2F_i^p + AF_i^{\mathrm{O}}) \implies \sigma_{\nu\mathrm{H_2O}} = \frac{1}{2+A}(2\sigma_{\nu p} + A\sigma_{\nu\mathrm{O}}),$$

  with $A = 16$ and the isoscalar $Z = N = 8$ for O nucleus.
- We define the nuclear corrections as the cross section ratios [following BGR]

$$R_{\mathrm{O}} = \frac{\sigma_{\nu\mathrm{O}}}{\sigma_{\nu I}},$$

  where I is the isoscalar. The nucleus cross section $\sigma_{\nu\mathrm{O}}$ are obtained with nuclear PDFs.
- The final H_2O-averaged cross section can be obtained through

$$\sigma_{\nu\mathrm{H_2O}} = \sigma_{\nu I} R_{\mathrm{O}} R_{\mathrm{H_2O}/O},\ R_{\mathrm{H_2O/O}} = \frac{2\sigma_{\nu p} + A\sigma_{\nu\mathrm{O}}}{2+A}/\sigma_{\nu\mathrm{O}}.$$

  with uncertainty propagated as

$$\frac{\delta\sigma_{\nu\mathrm{H_2O}}}{\sigma_{\nu\mathrm{H_2O}}} = \sqrt{\left(\frac{\delta\sigma_{\nu I}}{\sigma_{\nu I}}\right)^2 + \left(\frac{A}{2+A}\frac{\delta R_{\mathrm{O}}}{R_{\mathrm{O}}}\right)^2}.$$

- We provide $\sigma_{\nu I}$, R_{O} and $R_{\mathrm{H_2O/O}}$ as numerical tables [2303.13607].
- Many other impacts can be explored in more details, such as target-mass [2301.07715], off-shell corrections [1704.00204], etc.

Nuclear effects on PDFs

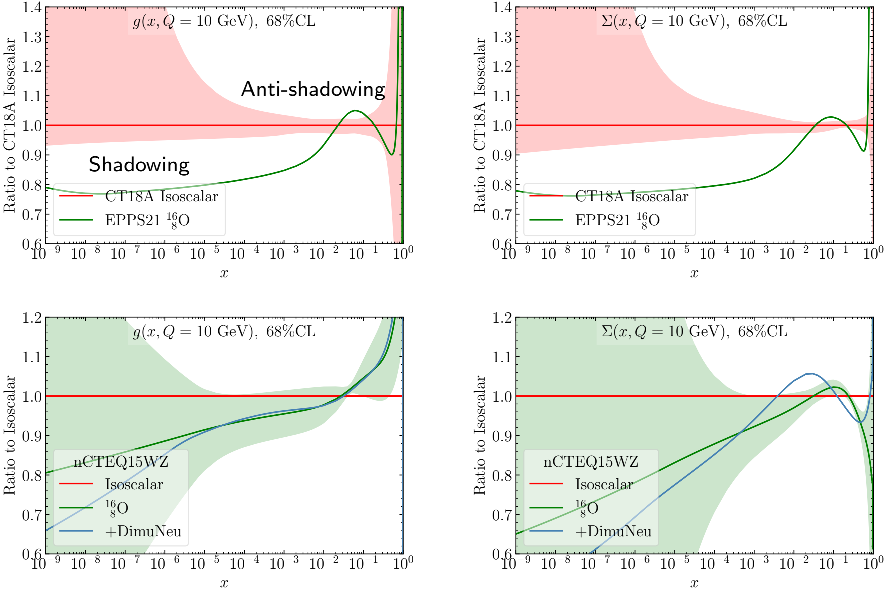

Neutrino scatterign with Oxygen and water

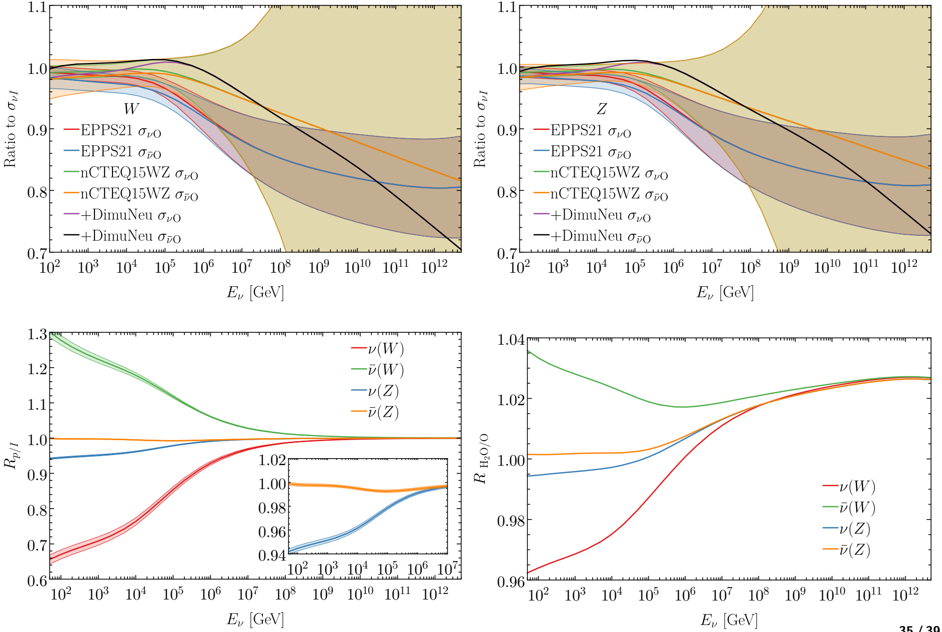

A comparison again

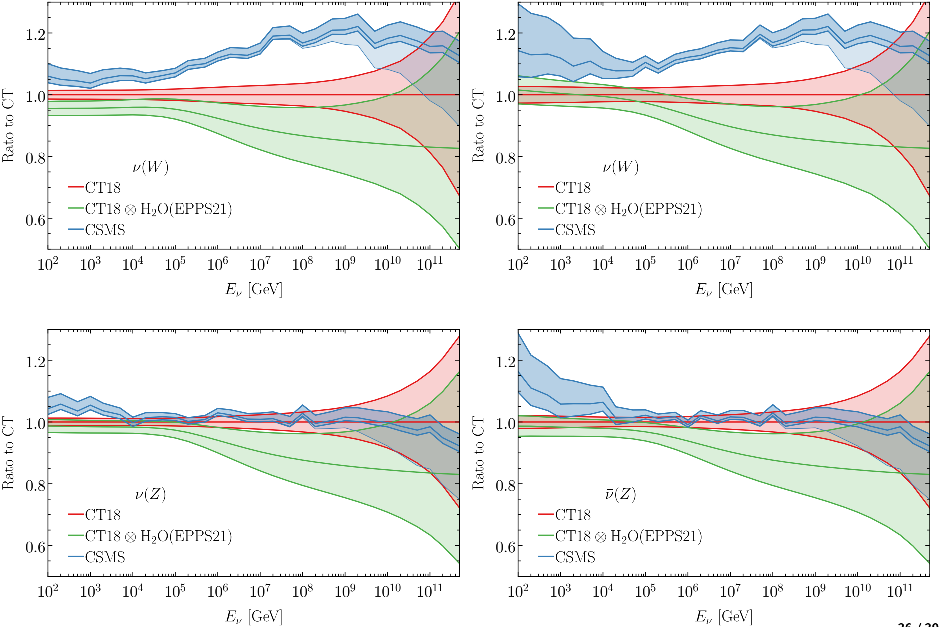

Compare with IceCube data

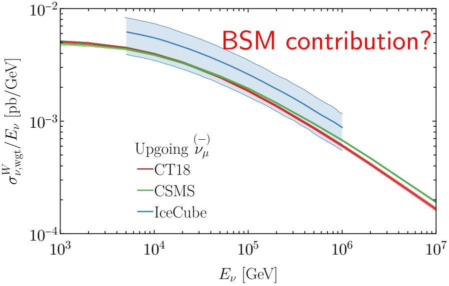

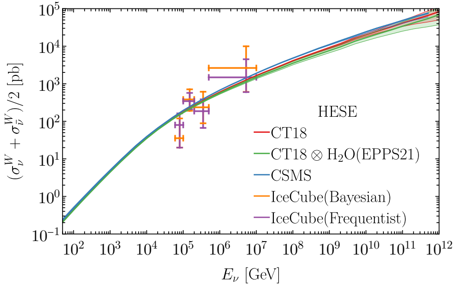

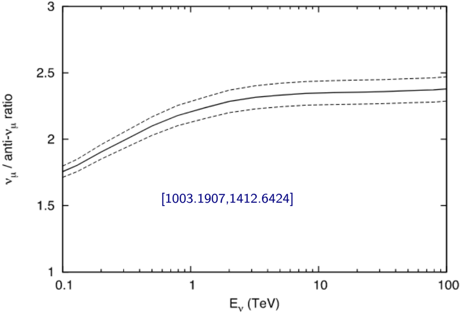

- The absorption cross section [IceCube, Nature 17'] is weighted with neutrino flux.

$$\sigma_{\nu,\mathrm{wgt}} = \frac{\Phi_\nu \sigma_\nu + \Phi_{\bar\nu}\sigma_{\bar\nu}}{\Phi_\nu + \Phi_{\bar\nu}}.$$

- the HESE cross section is averaged [IceCube, PRD20'].

Accelerator neutrinos and energy gap

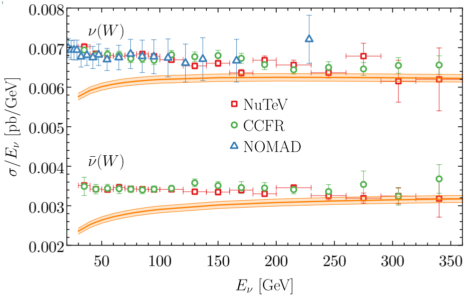

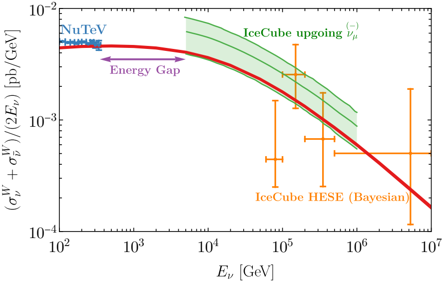

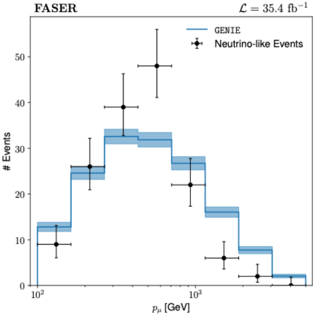

- At low E_ν, the missing Quasi-Elastic (QE) scattering and Resonance (RES) production become important.
- The energy gap can be potentially filled by the FASER (FPF) measurements.
- First FASER measurement comes out [2303.14185].

Conclusion

- We have performed a state-of-art calculation for high-energy neutrino-nucleon scattering.
- Partons have been included up to $n_f = 6$ flavors (4%).
- The perturbative QCD order has been achieved up to exact NNLO (heavy-quark mass effect –2%), and zero-mass N3LO (3%).
- Small-x resummation has been included with the BFKL equation (20%).
- Nuclear effects have been explored with the nuclear PDF approach (20%).
- The PDF uncertainty varies from 1% to 70%.
- Our calculation provides a good description of neutrino DIS data, both for accelerator and astrophysical sources.
- The energy gap between IceCube and accelerator sources can be filled by the FASER (FPF) experiment.

The Earth absorption

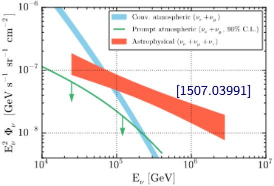

- At high E_ν, astrophysical neutrinos dominate.
- Single-power-law astro. flux

$$\frac{\mathrm{d}\Phi_{6\nu}}{\mathrm{d}E_\nu} = \Phi_{\mathrm{astro}} \left(\frac{E_\nu}{100\ \mathrm{TeV}} \right)^{-\gamma_{\mathrm{astro}}} \cdot 10^{-18} \mathrm{GeV}^{-1} \mathrm{cm}^{-2} \mathrm{s}^{-1} \mathrm{sr}^{-1}, \tag{14}$$

- The upward-going events (from northern sky)

$$\frac{\mathrm{d}N_{\mathrm{evt}}}{\mathrm{d}E_\nu} = \sigma_\nu^W \frac{\mathrm{d}\Phi_{6\nu}}{\mathrm{d}E_\nu} \mathscr{P}_{\mathrm{trans}} \tag{15}$$

- The transmission probability

$$\mathscr{P}_{\mathrm{trans}} \sim \exp\{-L(\theta)/\lambda(E_\nu)\} = \exp\{-L(\theta)\kappa\sigma(E_\nu)\} \tag{16}$$

- Earth model: isotopic abundance and density

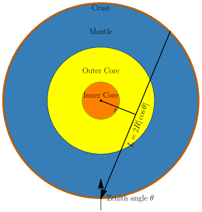

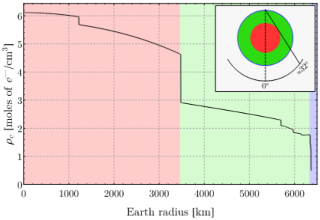

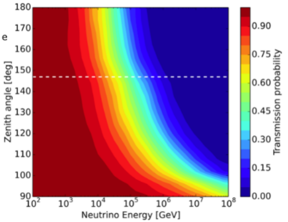

The transmission probability

- We take a spherical earth model, with the density from Preliminary Reference Earth Model (PREM) [Dziewonski&Anderson, 1981].
- The transmission probability
  $\mathscr{P}_{\rm trans}(E_\nu,\theta) = \Pi_{\Delta z} P_{\alpha\alpha}(E_\nu,\Delta z)\exp\{-\Delta z/\lambda(r,E_\nu)\}$,
  where the oscillation probability is $P_{\alpha\alpha} \approx 1$ when $E_\nu \gtrsim 1$ TeV, and the mean-free path $\lambda = 1/n_N(r)\sigma_\nu(E_\nu)$.

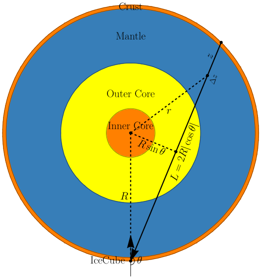

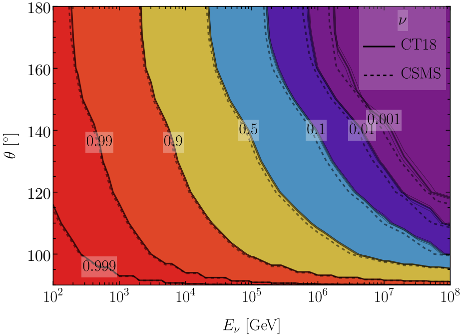

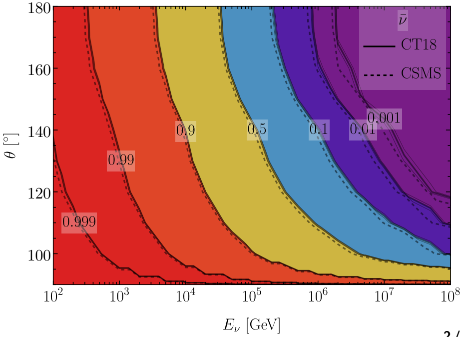

$(x_{\min}, Q_{\min})$ for $\bar{\nu}$ cross section

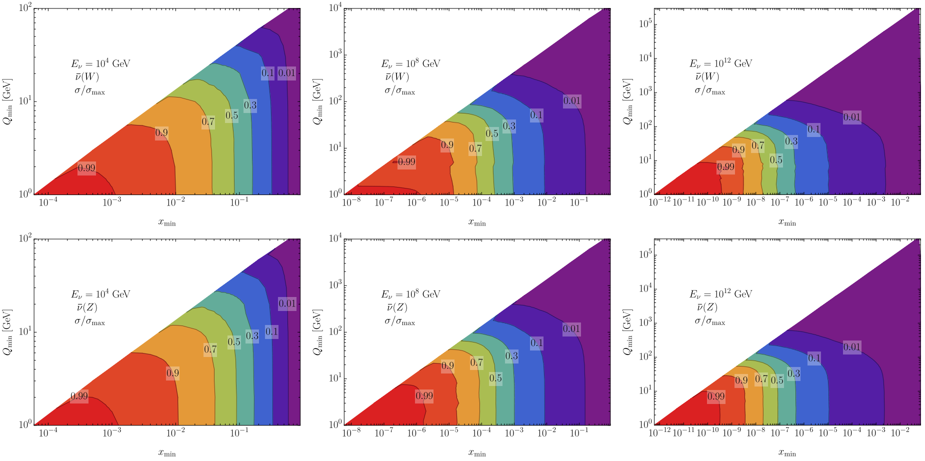

The CSMS and BGR calculations